DNA demethylation of inflammasome-associated genes is enhanced in patients with cryopyrin-associated periodic syndromes

Roser Vento-Tormo, PhD,[a]* Damiana Álvarez-Errico, PhD,[a]* Antonio Garcia-Gomez, PhD,[a] José Hernández-Rodríguez, MD, PhD,[b] Segundo Buján, MD, PhD,[c] Maria Basagaña, MD, PhD,[d] Maria Méndez, MD,[e] Jordi Yagüe, MD, PhD,[f] Manel Juan, MD, PhD,[f] Juan I. Aróstegui, MD, PhD,[f] and Esteban Ballestar, PhD[a] *Barcelona and Badalona, Spain*

Background: Inflammasomes are cytosolic multiprotein complexes in macrophages. They assemble after infection- or stress-associated stimuli, activating both caspase-1–mediated inflammatory cytokine secretion and pyroptosis. Increased inflammasome activity resulting from gene mutations is related to monogenic autoinflammatory syndromes. However, variable penetrance among patients with the same gene mutations suggests involvement of additional mechanisms associated with inflammasome gene regulation.

Objective: We sought to investigate the role of DNA demethylation in activating inflammasome genes during macrophage differentiation and monocyte activation in healthy control subjects and patients with autoinflammatory syndrome.

Methods: Inflammasome-related genes were tested for DNA methylation and mRNA levels by using bisulfite pyrosequencing and quantitative RT-PCR in monocytes *in vitro* differentiated to macrophages and exposed to inflammatory conditions. The contribution of Tet methylcytosine dioxygenase 2 (TET2) and nuclear factor κB to DNA demethylation was tested by using chromatin immunoprecipitation, small interfering RNA–mediated downregulation, and pharmacologic inhibition.

Results: We observed that inflammasome-related genes are rapidly demethylated in both monocyte-to-macrophage differentiation and on monocyte activation. Demethylation associates with increased gene expression, and both mechanisms are impaired when TET2 and nuclear factor κB are downregulated. We analyzed DNA methylation levels of inflammasome-related genes in patients with cryopyrin-associated periodic syndromes (CAPS) and familial Mediterranean fever, 2 archetypical monogenic autoinflammatory syndromes. Under the above conditions, monocytes from untreated patients with CAPS undergo more efficient DNA demethylation than those of healthy subjects. Interestingly, patients with CAPS treated with anti–IL-1 drugs display methylation levels similar to those of healthy control subjects.

Conclusion: Our study is the first to demonstrate the involvement of DNA methylation–associated alterations in patients with monogenic autoinflammatory disease and opens up possibilities for novel clinical markers. (J Allergy Clin Immunol 2016;■■■:■■■-■■■.)

Key words: *Cryopyrin-associated periodic syndromes, familial Mediterranean fever, autoinflammatory diseases, inflammasome, epigenetics, DNA methylation, active demethylation*

Innate immune myeloid cells, such as monocytes and macrophages, are crucial effectors and regulators of inflammation, and they are also involved in the maintenance of tissue homeostasis.[1] In response to inflammatory signals (eg, bacterial infection[2]), circulating monocytes extravasate and reach inflamed tissues, where they terminally differentiate into macrophages. Monocyte-to-macrophage differentiation can be recapitulated *in vitro* by exposing cells to GM-CSF or macrophage colony-stimulating factor (M-CSF),[3] with *in vitro*–differentiated GM-CSF–exposed macrophages producing larger amounts of proinflammatory cytokines than M-CSF–exposed macrophages. Moreover, monocytes themselves can respond to inflammatory cytokines, such as IL-1β, which promote their activation.

A crucial component of the monocyte/macrophage defense against microbial pathogens and endogenous danger signals is the inflammasome. Inflammasomes are multimeric complexes that assemble in the cytosol after sensing pathogens or danger-associated molecular patterns (eg, endogenous ATP or uric acid).[4] Once assembled, the inflammasome recruits and activates caspase-1 (CASP-1) and is thereby able to produce active forms of IL-1β and IL-18, inducing an inflammatory form of cell death known as pyroptosis.[5]

From [a]the Chromatin and Disease Group, Cancer Epigenetics and Biology Programme (PEBC), Bellvitge Biomedical Research Institute (IDIBELL), L'Hospitalet de Llobregat, Barcelona; [b]the Autoinflammatory Diseases Clinical Unit and Vasculitis Research Unit, Department of Autoimmune Diseases, Hospital Clinic, IDIBAPS, Barcelona; [c]Internal Medicine, Autoimmune and Systemic Diseases Services, Hospital Vall d'Hebron, Barcelona; [d]the Allergy Department and [e]the Department of Pediatrics, Hospital Universitari Germans Trias i Pujol, Universitat Autonoma de Barcelona, Badalona; and [f]the Department of Immunology-CDB, Hospital Clinic, IDIBAPS, Barcelona.

*These authors contributed equally to this work.

Supported by grant SAF2014-55942-R from the Instituto de Salud Carlos III, organisms ascribed to the Ministerio de Economía y Competitividad and cofunded by FEDER funds/European Regional Development Fund (ERDF)–a way to build Europe.

Disclosure of potential conflict of interest: J. I. Aróstegui has provided expert testimony for and received lecture fees from Swedish Orphan Biovitrum and has received research support and lecture fees from Novartis. E. Ballestar has received research support from Instituto de Salud Carlos III/Ministerio de Economía y Competitividad/FEDER (grant SAF2014-55942-R). The rest of the authors declare that they have no relevant conflicts of interest.

Received for publication January 11, 2016; revised April 6, 2016; accepted for publication May 9, 2016.

Corresponding authors: Esteban Ballestar, PhD, and Damiana Álvarez-Errico, PhD, Chromatin and Disease Group, Cancer Epigenetics and Biology Programme (PEBC), Bellvitge Biomedical Research Institute (IDIBELL), Avda. Gran Via 199-203, 08908 L'Hospitalet de Llobregat, Barcelona, Spain. E-mail: eballestar@idibell.cat. Or: dalvarez@idibell.cat.

0091-6749/$36.00

© 2016 American Academy of Allergy, Asthma & Immunology

http://dx.doi.org/10.1016/j.jaci.2016.05.016

Abbreviations used
AIM2: Absent in melanoma 2
ASC: Apoptosis-associated speck-like protein containing a caspase activation and recruitment domain
CAPS: Cryopyrin-associated periodic syndromes
CASP-1: Caspase-1
CBTB: Catalan Blood and Tissue Bank
ChIP: Chromatin immunoprecipitation
FMF: Familial Mediterranean fever
5hmC: 5-Hydroxymethylcytosine
M-CSF: Macrophage colony-stimulating factor
MSU: Monosodium urate
NF-κB: Nuclear factor κB
NLR: NOD-like receptor
qRT-PCR: Quantitative real-time PCR
siRNA: Small interfering RNA
TET2: Tet methylcytosine dioxygenase 2

Inflammasomes consist of a sensor molecule, an adaptor molecule, and the effector molecule CASP-1. The sensor molecules are either members of the NOD-like receptor (NLR) family or the absent in melanoma 2 (AIM2)–like receptor family.[4] The adaptor molecule apoptosis-associated speck-like protein containing a caspase activation and recruitment domain (ASC; encoded by *PYCARD*) contains specific domains needed for a proper interaction between sensor molecules and CASP-1. Once activated by the inflammasome, CASP-1 cleaves different inflammatory proteins (IL-1β, IL-18, and IL-33) into their bioactive forms.[6]

Related to these molecules, the IL-1 receptor antagonist (encoded by *IL1RN*) is a potent anti-inflammatory molecule that competes with IL-1α and IL-1β for IL-1 receptor binding.

The most extensively studied inflammasome is formed after oligomerization of NLRP3, ASC, and pro–CASP-1. Gain-of-function mutations in the *NLRP3* gene, also known as the cold-induced autoinflammatory syndrome 1 *(CIAS1)* gene, cause cryopyrin-associated periodic syndromes (CAPS). This monogenic autoinflammatory disease includes 3 phenotypes: familial cold autoinflammatory syndrome, Muckle-Wells syndrome, and neonatal-onset multisystem inflammatory disease. Autoinflammatory diseases are characterized by periodic or chronic episodes of systemic inflammatory attacks in the absence of infection or autoimmune disease. Currently, more than 20 genes have been found to be associated with different monogenic autoinflammatory diseases,[7] including the *MEFV* gene, which encodes the pyrin protein that is mutated in familial Mediterranean fever (FMF), and the *PSTPIP1* gene, which is mutated in patients with pyogenic sterile arthritis, pyoderma gangrenosum, and acne syndrome.

Despite the well-established genetic nature of these diseases, their penetrance varies, probably as a consequence of factors beyond the specific genetic defect. This is exemplified by the fact that autoinflammatory diseases can develop in adults, who are generally characterized by milder clinical features and higher frequency of low-penetrance mutations than pediatric patients.[8] It is likely that epigenetic alterations contribute to the pathogenesis and final clinical phenotype of these diseases.

Epigenetic marks, including methylation at cytosines followed by guanines (CpGs) and histone posttranslational modifications, are associated with gene expression status. Epigenetic changes are essential in cell differentiation. Specifically, genes relevant to macrophage function become demethylated (and overexpressed) during monocyte-to-macrophage differentiation.[9] By re-examining data from our previous study (GEO Series accession no. GSE71837),[10] we found that several inflammasome-related genes demethylate during monocyte-to-macrophage differentiation, which suggests that DNA methylation has a relationship with their transcriptional status. For this reason, we hypothesized that these genes display an aberrant methylation status in monocytes and macrophages of patients with autoinflammatory diseases compared with those from healthy subjects. The present study investigated whether these regulatory marks were altered in the context of these diseases.

METHODS

Isolation of peripheral blood monocytes and differentiation and activation experiments

Human blood samples from healthy control subjects were obtained as buffy coats from the Catalan Blood and Tissue Bank (CBTB). Anonymous healthy donors received oral and written information about the possibility that their blood would be used for research purposes. Before obtaining the first blood sample, all donors signed a consent form at the CBTB. The CBTB follows the principles set out in the World Medical Association Declaration of Helsinki. Blood samples corresponding to patients with CAPS and those with FMF came from Hospital Clínic, Hospital Vall d'Hebron and Hospital Universitari Germans Trias i Pujol in Barcelona. Participating clinicians gained approval from their corresponding ethics committees, and patients provided signed informed consent.

PBMCs were isolated by using a Ficoll-Paque gradient (Amersham, Buckinghamshire, United Kingdom). Pure monocytes were isolated from PBMCs by using positive selection with MACS magnetic CD14 antibody (Miltenyi Biotec, Bergisch Gladbach, Germany). Cells were then resuspended in RPMI 1640 (1×) plus GlutaMAXTM-1 (Gibco, Life Technologies, Carlsbad, Calif) containing 10% FBS, 100 U/mL penicillin, and 100 μg/mL streptomycin. For macrophage differentiation, medium was supplemented with 800 U of GM-CSF (Gentaur Molecular Products, Kampenhout, Belgium) over the course of 4 days and activated with 1 μg/mL LPS (Sigma-Aldrich, St Louis, Mo) for 24 hours. Monocytes were also activated either with LPS (1 μg/mL, Sigma-Aldrich) or IL-1β (10 ng/mL; PeproTech, Rocky Hill, NJ), and samples were harvested at various time points between 0 and 24 hours.

Bisulfite sequencing and pyrosequencing

Bisulfite modification of genomic DNA isolated from monocytes and macrophages was performed by using standard methods with biological triplicates. Oxidative bisulfite modifications were performed, as described by Booth et al.[11] Briefly, 2 μL of the converted DNA (approximately 20-30 ng) was used as a template in each subsequent PCR. Primers for PCR amplification and sequencing were designed with the PyroMark Assay Design 2.0 software (Qiagen, Hilden, Germany). PCRs were performed with the HotStart Taq DNA polymerase PCR kit (Qiagen), and the success of amplification was assessed by means of agarose gel electrophoresis. PCR products were pyrosequenced with the PyroMark Q24 system (Qiagen). Primer sequences are listed in Table E1 in this article's Online Repository at www.jacionline.org.

Quantitative real-time PCR

For quantitative real-time PCR (qRT-PCR), cDNA was produced with SuperScript II Reverse Transcriptase (Invitrogen, Carlsbad, Calif). qRT-PCR was done on a LightCycler 480 II System using LightCycler 480 SYBR Green Mix (Roche, Basel, Switzerland). Reactions were carried out in triplicate, and qRT-PCR data were analyzed by using the standard curve method. Data were normalized against the housekeeping genes ribosomal protein L38 (*RPL38*) and hypoxanthine phosphoribosyltransferase 1 (*HPRT1*), which were used as controls. Primer sequences are listed in Table E1.

Transfection of primary human monocytes

We used ON-TARGETplus small interfering RNAs (siRNAs) against Tet methylcytosine dioxygenase 2 (TET2) to perform knockdown experiments in peripheral blood monocytes. We also used the ON-TARGETplus Non-targeting Control Pool as a negative control. We transfected monocytes with siRNAs using Lipofectamine 3000 Reagent (Thermo Fisher Scientific, Carlsbad, Calif) and added 800 U of GM-CSF (Gentaur Molecular Products) 24 hours later. We examined TET2 levels by using Western blotting (reference: MABE462; Millipore, Billerica, Mass) 4 days after GM-CSF addition (5 days after transfection).

Putative binding of nuclear factor κB motifs

The possible occurrence of nuclear factor κB (NF-κB) subunit binding motifs in the region comprising 1500 bp around the transcription start site was inspected by using ConSite matrices.

Chromatin immunoprecipitation assays

For chromatin immunoprecipitation (ChIP) assays, $CD14^+$ cells (monocytes) treated with GM-CSF, IL-1β, or LPS at various time points between 0 and 24 hours were crosslinked with 1% formaldehyde over 15 minutes and subjected to immunoprecipitation after sonication by using a Covaris ultrasonicator (Covaris, Woburn, Mass). ChIP experiments were performed with the low-cell ChIP kit protein A (Diagenode SA, Seraing, Belgium). We used a rabbit polyclonal antibody against the carboxyl-terminal end of NF-κB p65 (sc-372; Santa Cruz Biotechnology, Heidelberg, Germany). Immunoprecipitated material was used to analyze specific sequences by using qRT-PCR (see primer sequences in Table E1).

Apoptosis assay

To quantitate apoptosis, we used the fluorescein isothiocyanate Annexin V Apoptosis Detection Kit II (BD Biosciences, San Jose, Calif). Monocytes were cultured with GM-CSF, IL-1β, or LPS alone or in combination with monosodium urate (MSU) crystals and ATP over 24 hours. As a positive control, monocytes were cultured with 10 μmol/L camptothecin for 4 hours. Approximately 1×10^6 cells/mL were stained with Annexin V conjugated with fluorescein isothiocyanate and propidium iodide and processed on a Gallios Flow Cytometer (Beckman Coulter, Pasadena, Calif) and subsequently analyzed by using FlowJo software (Tree Star, Ashland, Ore).

Cytokine detection

Supernatants from 24-hour LPS-activated GM-CSF–exposed macrophages were collected, and IL-1β, IL-6, IL-8, and TNF-α levels were measured by using the Cytokine Human Ultrasensitive MultiPlex Panel for Luminex Platform (Thermo Fisher Scientific), according to the manufacturer's instructions.

Statistical analysis

Statistical significance of the differences in methylation levels of healthy control subjects and patients with CAPS or those with FMF was evaluated by using the paired *t* test (for direct comparison of methylation percentages between monocytes before/after stimulation) and Mann-Whitney *U* test (for the comparison of ratios between healthy control subjects vs patients with CAPS or those with FMF at the indicated conditions; GraphPad Prism 6; GraphPad Software, La Jolla, Calif). Differences were considered significant at a P value less than .05.

RESULTS

DNA demethylation signature of inflammasome-associated genes during monocyte-to-macrophage differentiation

The examination of DNA methylation changes in primary human monocyte-to-macrophage GM-CSF–mediated differentiation (followed by LPS-mediated activation) revealed loss of methylation at thousands of CpG sites (GSE71837).[10] Among the functional categories significantly enriched when performing gene ontology analysis of the demethylated CpG sites, we identified several categories relevant to macrophage identity and function (inflammatory response [GO:0006954], $P = 8.1e\text{-}08$; innate immune response [GO:0045087], $P = 7.8e\text{-}08$). Specifically, we identified within these categories several genes related to the inflammasome (*AIM2*, *NLRC5*, *PYCARD*, *CASP1*, and *PSTPIP2*) or its targets (*IL1A*, *IL1B*, and *IL1RN*; Fig 1, *A*, top; GSE71837), for which demethylation was accompanied by subsequent activation of gene expression (Fig 1, *A*, bottom; GSE75938). Bisulfite pyrosequencing of these CpG sites during monocyte-to-macrophage differentiation confirmed these changes over time (Fig 1, *B*). In some cases, such as with *IL1B*, changes were very fast, and greater than 80% demethylation occurred within 24 hours after exposure to GM-CSF (Fig 1, *B*). Other genes (*IL1RN*, *NLRC5*, and *AIM2*) displayed more gradual methylation changes. In these analyses we included control genes that did not become demethylated during monocyte-to-macrophage differentiation, such as *DUOX1*.[10]

In parallel, we also checked expression changes of these inflammasome-associated genes over time. Several genes, including *IL1A*, *IL1B*, *AIM2*, and *NLRC5*, underwent an increase in mRNA levels but only after LPS-mediated activation, whereas others (*IL1RN* and *PSTPIP2*) were concomitantly activated as demethylation progressed (Fig 1, *B*).

To further explore how increased expression of these genes depends on DNA demethylation, we downregulated TET2. TET2 participates in active demethylation in monocytes[12] through the generation of oxidized intermediates of 5-metylcytosine, such as 5-hydroxymethylcytosine (5hmC). Therefore we performed siRNA experiments to obtain efficient downregulation of TET2 (Fig 1, *C*) and tested the effects on the demethylation and upregulation of inflammasome genes using *DUOX1* as a control gene. We observed partial impairment of demethylation after TET2 depletion (Fig 1, *D*). Accumulation of 5hmC, which occurs on monocyte stimulation with GM-CSF, also decreased after TET2 downregulation (Fig 1, *D*). Analysis of the mRNA levels of these genes by using qRT-PCR showed that downregulation of TET2 also resulted in decreased upregulation (Fig 1, *E*), revealing that inflammasome-associated genes depend on TET2-mediated demethylation for activation.

Finally, we performed Luminex assays to measure the levels of inflammatory cytokine IL-1β released into the medium on LPS activation of macrophages and to test the effects of TET2 downregulation. Our results showed a dependence on TET2 in the ability of GM-CSF–exposed macrophages to produce and secrete bioactive IL-1β directly linked to TET2 levels (Fig 1, *F*), although other measured cytokines showed different behavior (TNF-α increased production after TET2 inhibition, and no changes of IL-8 secretion were detected).

Direct stimulation of the inflammasome in monocytes results in active demethylation of *IL1B*, *IL1RN*, and *CASP1*

Our results demonstrated that expression of several inflammasome genes depends on TET2-mediated DNA demethylation in GM-CSF–mediated monocyte-to-macrophage differentiation. This prompted us to evaluate demethylation of such genes in monocytes exposed to inflammatory conditions. To this end, we

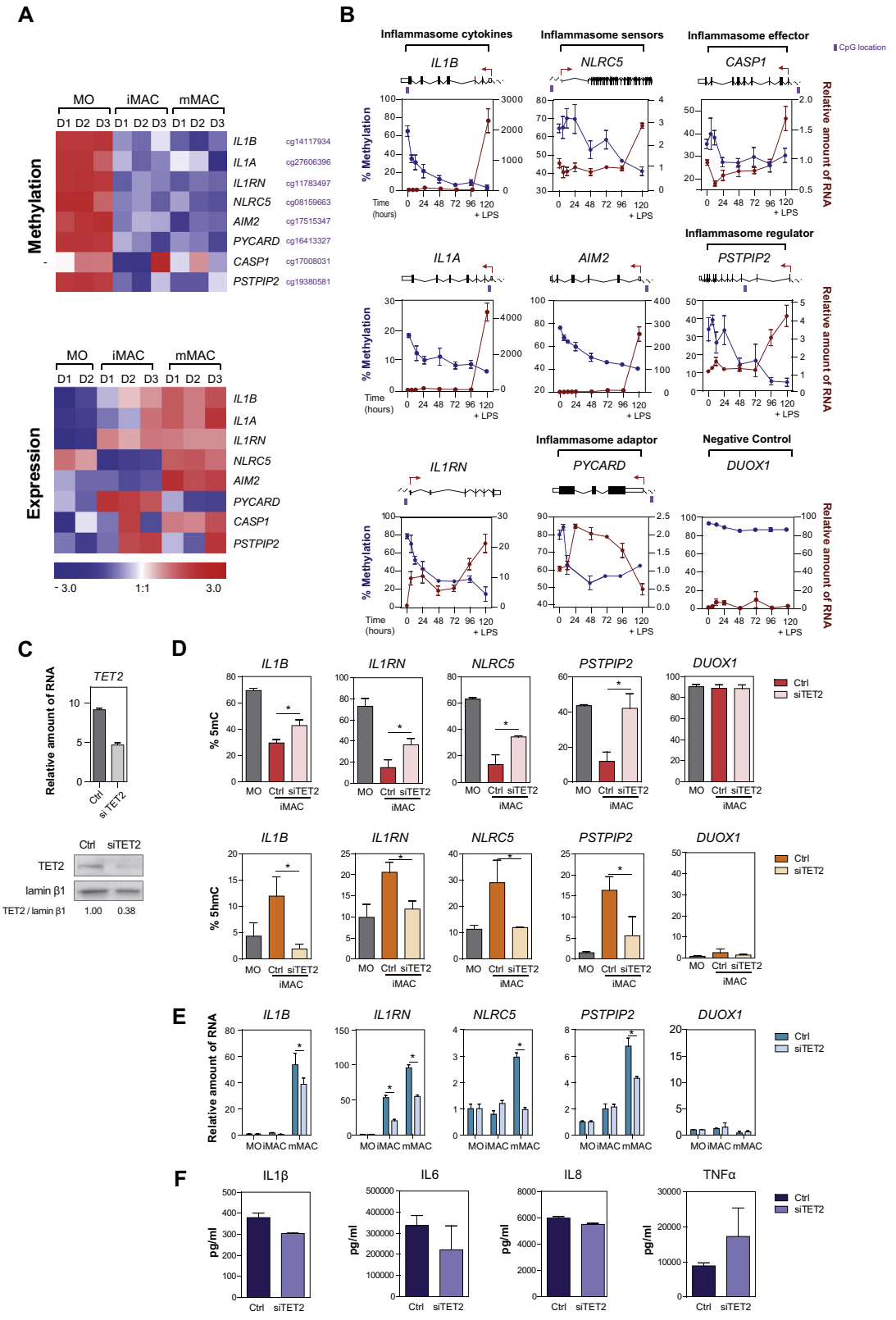

FIG 1. Inflammasome genes undergo DNA demethylation during GM-CSF–mediated monocyte-to-macrophage differentiation. **A,** Heat maps represent normalized β values for DNA methylation *(top)* and gene expression values *(bottom)* in arbitrary units for inflammasome-related genes in monocytes, immature macrophages, and mature macrophage Illumina CpG coordinates are shown next to each gene name. **B,** Bisulfite pyrosequencing showing DNA methylation dynamics *(blue line)* and qRT-PCR expression data normalized to *HPRT1* and *RPL38 (red line)*. A scheme of each gene showing the transcription start site

compared the DNA methylation changes in monocytes under exposure to IL-1β (10 ng/mL) and LPS (1000 ng/mL) over a period of 24 hours. We used LPS alone; in combination with NLRP3 inflammasome inducers, such as MSU crystals (200 ng/mL)[13]; or in the presence of ATP (1 mmol/L).[14] These conditions were compared with the exposure of monocytes to GM-CSF. Given that monocytes spontaneously attach to culture plates and differentiate to macrophages, even in the absence of stimulation, we also performed parallel experiments to test all the above conditions in the presence of poly-2-hydroxyethyl methacrylate to minimize the adherence of monocytes to the plates.

To test whether these conditions induce apoptosis or necrosis, we performed flow cytometric analysis using Annexin V and propidium iodide staining, with exposure to camptothecin as a positive control of apoptosis (Fig 2, *A*). We observed that GM-CSF and IL-1β did not stimulate apoptosis.

After exposure of monocytes to these different stimuli, we performed bisulfite pyrosequencing and qRT-PCR of inflammasome-associated genes. As controls, we also analyzed *DUOX1* and *MITF*, genes that undergo demethylation during monocyte-to-macrophage differentiation but are not linked to inflammation. Both LPS and IL-1β stimulation resulted in demethylation of inflammasome-associated genes, such as *IL1B*, *IL1A*, *IL1RN*, and *CASP1*, over a 24-hour period (Fig 2, *B*). Our results were consistent with the ability of MSU crystals to enhance the LPS-induced release of IL-1β by monocytes through a CASP-1–mediated process.[15] Demethylation associated with IL-1β or LPS stimulation only affected inflammasome genes (Fig 2, *B*). We obtained similar results with monocytes exposed to IL-1β in the presence of poly-2-hydroxyethyl methacrylate, which prevented the attachment of monocytes to the culture plates (see Fig E1, *A*, in this article's Online Repository at www.jacionline.org). Direct stimulation of monocytes was associated with a peak of increased mRNA levels around 3 to 6 hours after stimulation (Fig 2, *C*) for inflammasome-associated genes, such as *IL1A*, *IL1B*, *IL1RN*, and *CASP1*, whereas control genes (*DUOX1* or *MITF*) displayed different expression dynamics. In the case of genes such as *IL1A* and *IL1RN*, this peak in expression coincided with an increase in 5hmC levels (see Fig E1, *B*). Other genes, such as *AIM2* and *PYCARD*, did not display an increase in mRNA levels during the first 24 hours (see Fig E1, *C*), suggesting alternative mechanisms for these 2 genes under LPS- and IL-1β–mediated monocyte activation.

We also observed that camptothecin-induced apoptosis did not result in demethylation of inflammasome-associated genes, such as *IL1B* or *AIM2* (see Fig E1, *D*), reinforcing the notion that the observed demethylation is independent of apoptosis.

NF-κB mediates demethylation of inflammasome-associated genes

Toll-like receptor– or IL-1 receptor–initiated signals are known to generate strong NF-κB–mediated responses in monocytes and macrophages. Analysis of the sequences in a 1500-bp window around the transcription start site of inflammasome-associated demethylated genes showed the presence of NF-κB p65 subunit binding sites (Fig 3, *A*). To investigate the involvement of NF-κB in the DNA demethylation process affecting inflammasome genes, we first treated monocytes with the NF-κB inhibitor Bay 11-7082 and investigated its effects on the DNA methylation changes of inflammasome-associated genes under different conditions (GM-CSF, IL-1β, and LPS in the absence or presence of MSU and ATP). Bay 11-7082 reduces the levels of phosphorylated Ser536 of p65, which corresponds to its active form. We tested concentrations similar to those previously used[16] and selected 10 μmol/L for Bay 11-7082. The phosphorylation of p65 observed after IL-1β or LPS stimulation of monocytes decreased in the presence of Bay 11-7082 (Fig 3, *B*). We then performed bisulfite pyrosequencing to measure the effects of this NF-κB inhibitor on the DNA methylation levels of inflammasome-associated genes. Bay 11-7082 dramatically impaired DNA demethylation in all cases (Fig 3, *C*). Control genes not associated with inflammation, such as *DUOX1*, did not show any effect (Fig 3, *C*). These effects were also noted at the expression level (Fig 3, *D*).

To test the potential direct effect of NF-κB on these methylation changes, we performed ChIP assays to assess the binding of NF-κB subunit p65 to inflammasome genes. We confirmed the specific binding of NF-κB p65 to genes, such as *IL1B*, *IL1A*, *IL1RN*, and *CASP1* (and the absence of binding to unrelated control genes, such as the myogenic regulatory gene *MYOD1*; Fig 3, *E*), after stimulation with IL-1β and LPS, reinforcing the notion that NF-κB participates in their regulation.

Patients with CAPS not treated with anti–IL-1 drugs are more prone to demethylation of inflammasome genes than healthy control subjects and treated patients

The ability of inflammasome-associated genes to demethylate and activate provides a potential mechanism that could be dysregulated under certain conditions, such as monogenic autoinflammatory diseases, including CAPS and FMF.

Therefore we examined the demethylation of inflammasome-related genes in monocytes to macrophages after stimulation by GM-CSF under the aforementioned inflammatory conditions in the presence of IL-1β in a small cohort of patients with CAPS (n = 17), patients with FMF (n = 5), and healthy control subjects (n = 21). Patients with CAPS and FMF displayed *bona fide* mutations (see Table E2 in this article's Online Repository at www.jacionline.org). For the group of patients with CAPS, 5 of 17 patients had not received anti–IL-1 treatment.

We observed that unstimulated monocytes from patients and healthy control subjects displayed virtually identical levels of DNA methylation for *IL1B*, *ILR1N*, *NLRC5*, AIM2, *PYCARD*, and *CASP1* (Fig 4 and Table E3 in this article's Online Repository

(*TSS*; *red arrow*) and the CpG site location *(below)* is included. **C,** qRT-PCR and Western blotting showing the effective downregulation of TET2 in monocytes at 96 hours. **D,** Analysis of 5-methylcytosine (*5mC*; *top)* and 5hmC *(bottom)* levels in TET2 siRNA–silenced immature macrophages performed by using combination of DNA bisulfite and oxidative bisulfite techniques (bisulfite = 5mC + 5hmC, oxidative bisulfite = 5mC) 5 days after transfection. **E,** qRT-PCR of inflammasome genes in siRNA-silenced TET2 immature macrophages. **F,** Cytokine levels after siRNA-mediated silencing of TET2 measured by using the Luminex assay. *iMAC,* Immature macrophage; *mMACs,* mature macrophage; *MO,* monocyte. *$P < .05$.

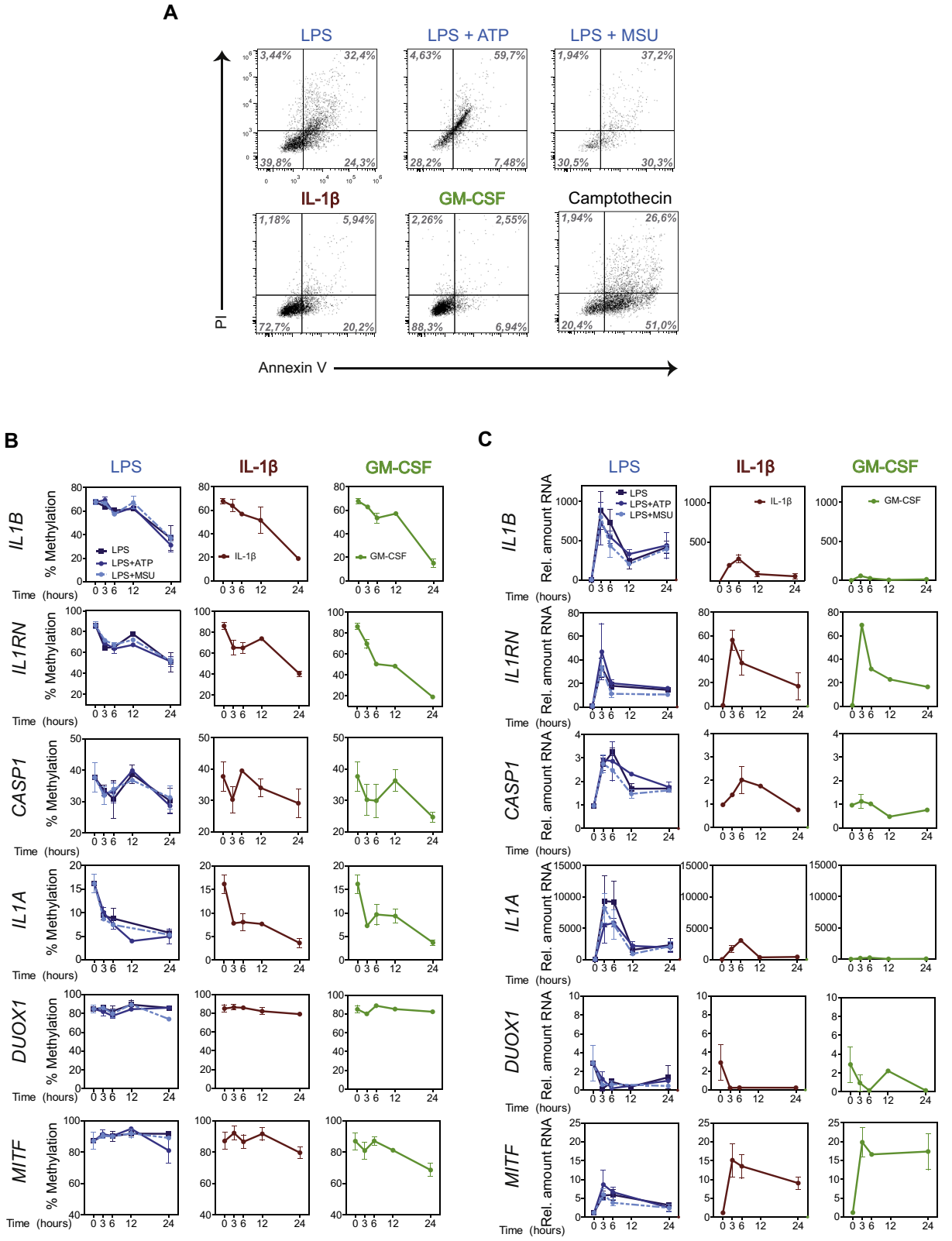

FIG 2. Inflammasome-related genes lose DNA methylation during LPS- and IL-1β–mediated monocyte activation. **A,** Annexin V and propidium iodide *(PI)* staining in monocytes 24 hours after the indicated stimulation. **B,** DNA methylation quantified by means of bisulfite pyrosequencing in monocytes cultured according to indicated conditions. *DUOX1* and *MITF* were used as controls. **C,** Changes in gene expression were determined by using qRT-PCR in monocytes cultured under the same conditions.

A

CONSITE (80%)

IL1B	-622(-);-**295(+)-294(-);+**504(-);+504(+)
IL1RN	-1444(-);-1431(-);-1431(+);-1386(+);-502(+); **-433(+);-432(-)**; +136(-)
AIM2	-560(+);-559(-);-559(+);-471(+);-1280(-);-944(-);-760(-);-760(+);-759(-);-560(-);-471(-);-470(-);-449(-)
NLRC5	-1326(-);-249(+);-28(-);-27(-);+220(-);+1192(+);+1235(+)
PSTPIP2	-30(+);+204(+);+205(-);+205(+);+670(+);+686(+);+803(+);+804(-);+804(+);+1314(+)
IL1A	-252(+); **-164(+);** +153(+); +811(-);+1222(+);+1259(-);
CASP1	**-1425(+);-1424(-);-1424(+);-1423(-)** ;-874(+);-784(-);-140(-);- 47(-);+555(+);+556(-);+556(+);+579(+)
PYCARD	-1449(+);-506(-);-506(+);-505(-);+196(+);+854(+);+855(-);+855(+);+885(-);+1026(+);+1148(-);+1215(-)

B

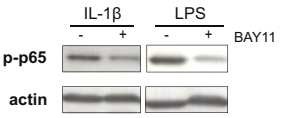

C

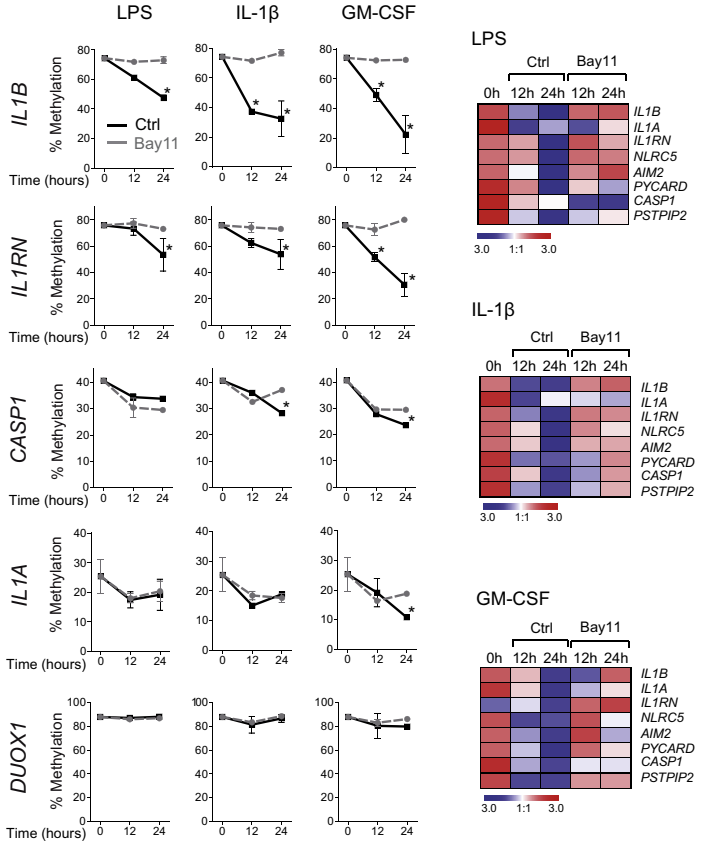

D

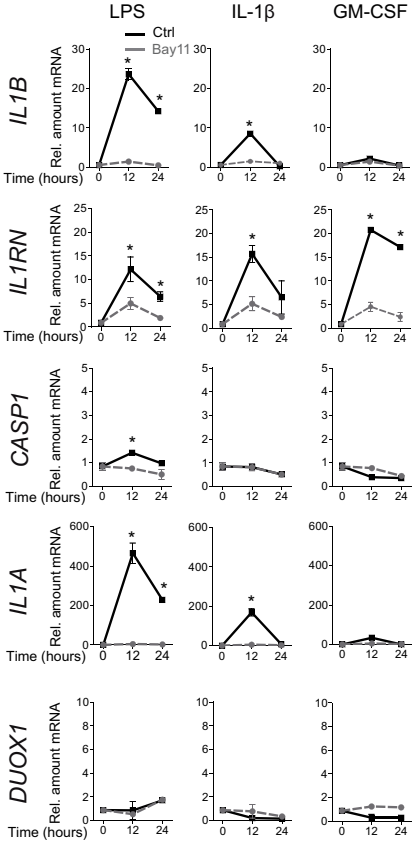

E

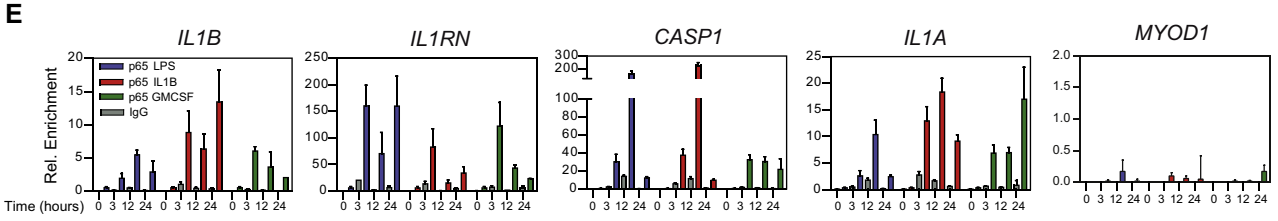

FIG 3. Contribution of the NF-κB pathway to inflammasome gene demethylation. **A,** ConSite prediction of p65 binding sites within ±1500 bp of the transcription start site. Regions selected for primers for ChIP assays are highlighted. **B,** Western blot analysis of p65 phosphorylation. **C,** Time-course bisulfite-modified DNA pyrosequencing showing DNA methylation changes of inflammasome genes on indicated stimuli in the presence or absence of the NF-κB inhibitor Bay 11-7082. Control subjects were treated with the same amount of dimethyl sulfoxide. Each *point* is the average of independent biological duplicates. The analyzed

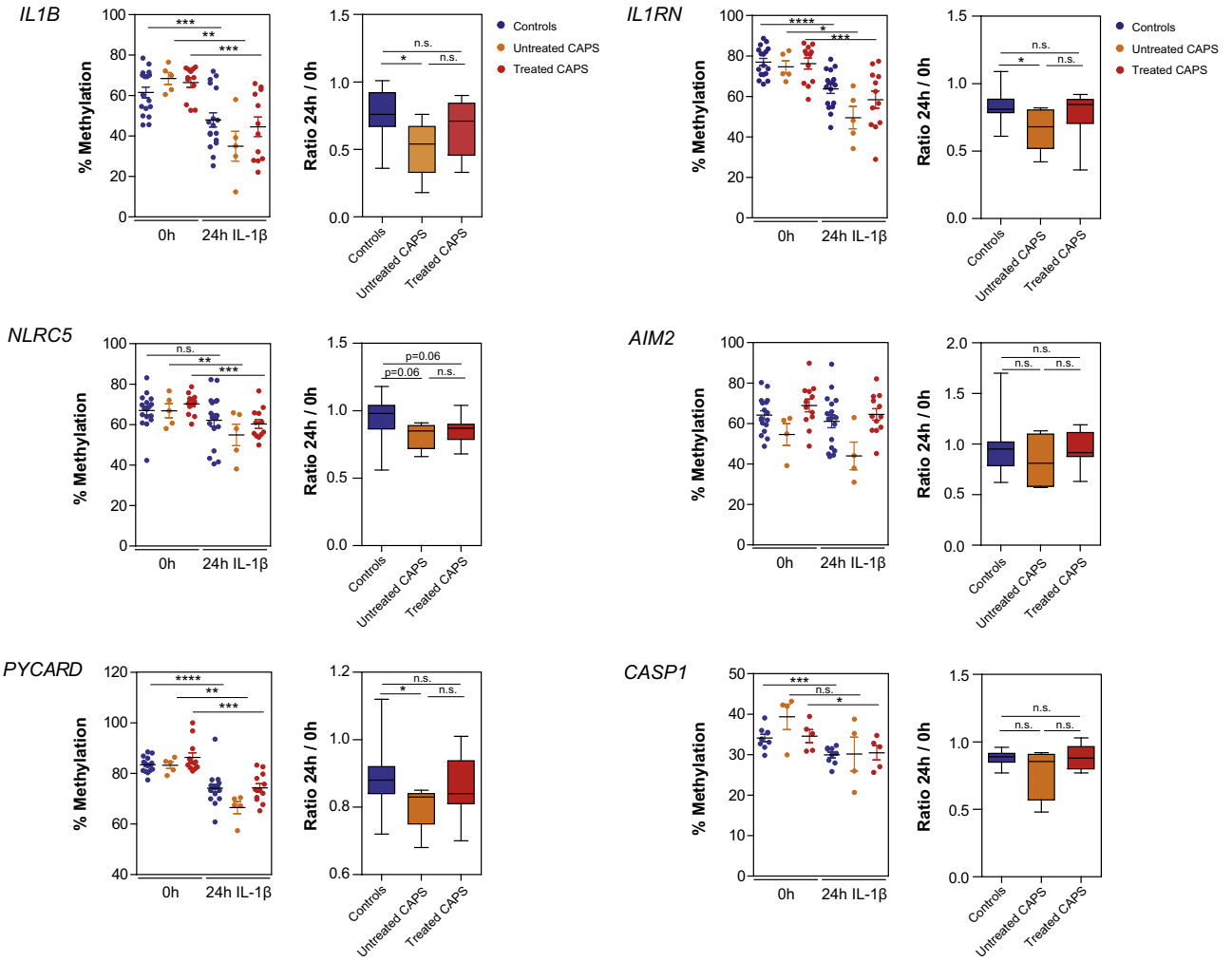

FIG 4. Demethylation of inflammasome genes in monocytes from patients with CAPS compared with those from healthy subjects. Methylation levels of monocytes before (0 hours) and after (24 hours) stimulation with IL-1β, as estimated by using bisulfite pyrosequencing, are shown. For each gene, demethylation is represented as the ratio between the methylation percentage of monocytes at 24 hours after IL-1β stimulation and before stimulation. Patients are divided into 2 groups: untreated and treated with anti–IL-1β drugs (details in Tables E2 and E3). The Mann-Whitney *U* and paired *t* tests were used for comparisons (as specified in the Methods section). **P* < .05, ***P* < .01, ****P* < .001, and *****P* < .0001. *n.s.*, Not significant.

at www.jacionline.org). However, we found that monocytes stimulated with IL-1β underwent significantly more efficient demethylation of *IL1B*, *IL1RN*, *NLRC5*, and *PYCARD* in patients with CAPS who had not been treated with anti–IL-1 therapy than in healthy control subjects (Fig 4). Patients with CAPS who received anti–IL-1 treatment did not display significant differences when compared with healthy control subjects, suggesting that the treatment might reverse the trend observed for patients with CAPS in the absence of such therapy. This trend was also apparent for monocytes stimulated with GM-CSF for 24 hours, although the comparison was only significant for the *IL1B* gene (see Fig E2, *A*, in this article's Online Repository at www.jacionline.org). In the case of patients with FMF, the results did not reach statistical significance, and no evident differences were observed (see Fig E2, *B*). To test whether the difference in untreated patients with CAPS was associated with differential upregulation of these genes, we performed qRT-PCR to quantitate their mRNA levels. We observed a trend for increased expression

gene is indicated on the *left*, and the treatments (LPS, IL-1β, and GM-CSF) are shown at the *top of each graph*. Heat maps for each treatment (LPS, IL-1β, and GM-CSF) summarizing methylation levels of genes at 12 and 24 hours of stimuli are depicted. **D,** Gains of gene expression for inflammasome-associated genes in the absence or presence of the NF-κB inhibitor Bay 11-7082, as analyzed by using qRT-PCR in monocytes cultured under previously described conditions. **E,** ChIP assays showing binding to indicated genes of the NF-κB p65 at 0, 3, 12, and 24 hours after stimulation of monocytes with IL-1β, LPS, and GM-CSF. Data are presented as relative enrichment (immunoprecipitated fraction divided by the input fraction). The *MYOD1* gene is used as a control gene. **P* < .05.

of genes, such as *IL1B* and *IL1RN*, in untreated patients with CAPS compared with healthy subjects and patients with CAPS treated with anti–IL-1β therapy, although the data did not reach statistical difference (see Fig E2, *C*) at 24 hours. However, we cannot discard the possibility that differences can occur under different dynamics than those obtained for DNA methylation.

In summary, our results indicate that stimulated monocytes from patients with CAPS have lower methylation levels for several inflammasome-related genes than their healthy counterparts and that IL-1 drugs could reverse that trend.

DISCUSSION

For the first time, our results identify the existence of TET2-dependent DNA demethylation for several inflammasome-related genes in monocyte-to-macrophage differentiation and monocytes under inflammatory conditions. The capacity of inflammasome-related genes to become demethylated is also dependent on NF-κB. We also report that the DNA methylation–dependent regulation of inflammasome product genes, notably *IL1B*, *IL1RN*, *NLRC5*, and *PYCARD*, is exacerbated in patients with CAPS who do not receive anti–IL-1 drugs and that treatment reverses such an effect, providing a potential source for useful clinical biomarkers.

Our study reports the relationship between DNA demethylation and upregulation of inflammasome-related genes in monocyte-to-macrophage differentiation and on direct Toll-like receptor– or IL-1 receptor–mediated stimulation of monocytes. In the case of GM-CSF–mediated monocyte-to-macrophage differentiation, genes like *IL1B*, *IL1A*, *NLRC5*, *AIM2*, and *CASP1* display DNA demethylation during the differentiation step before their increase in expression, which occurs only after LPS-mediated activation of macrophages. This suggests that DNA demethylation is a first and required step to guarantee the proper and fast response of the inflammasome. DNA demethylation is TET2 dependent, as demonstrated by the partial impairment of DNA demethylation and upregulation of gene expression and proper inflammasome-mediated response after TET2 downregulation, thus indicating the relevance of active DNA demethylation during the process.

In addition to demethylation during GM-CSF–stimulated monocyte-to-macrophage differentiation, inflammasome-related genes also become demethylated when monocytes are directly stimulated with LPS and IL-1β. Under these conditions, the dynamics of expression in relation to DNA demethylation vary with respect to the GM-CSF conditions, suggesting the participation of additional players, coexistent mechanisms, or both in the regulation of these genes.

Our results also confirm the involvement of NF-κB in DNA demethylation and the upregulation of inflammasome-related genes during monocyte activation. NF-κB can participate directly or indirectly in the recruitment of TET2, resulting in subsequent DNA demethylation. Additional experiments to explore the potential interaction between NF-κB subunits and TET2 are needed.

Finally, we have found that exacerbated DNA demethylation of several inflammasome-related genes (*IL1B*, *IL1RN*, *NLRC5*, and *PYCARD*) occurs in activated monocytes from untreated patients with CAPS compared with their healthy counterparts. DNA demethylation in patients with CAPS could set a lower threshold for IL-1β production, establishing a positive loop between IL-1β production and further inflammasome activation. Nonetheless, no basal differences in DNA methylation of the inflammasome-related genes are apparent in nonstimulated monocytes when comparing patients and healthy control subjects, and only IL-1β stimulation is capable of unveiling the difference between them. Thus high IL-1β levels would recapitulate the natural environment of monocytes in these IL-1β–driven diseases, enhancing DNA demethylation in patients with CAPS and causing a major induction of gene expression relative to control subjects.

In this study untreated patients with CAPS harboring different mutations (see Table E2) exhibited a similar methylation profile of IL-1β–stimulated monocytes in genes, such as *IL1B*, *ILR1N*, *NLRC5*, and *PYCARD*. These findings suggest that defects in the epigenetic control of these genes are independent of the specific mutation of the *NLRP3* gene, and perhaps enhanced demethylation is present in symptomatic patients who do not meet the genetic diagnostic criteria. In this sense the generation of high-throughput profiles of DNA methylation for these patients could provide further insight into the extent of methylation-related defects in patients with CAPS and evaluate the potential for additional diagnostic markers. It is remarkable that patients with CAPS undergoing anti–IL-1β treatment display demethylation levels in stimulated monocytes similar to those seen in healthy control subjects, suggesting the effectiveness of the drug in preventing the exacerbated demethylation of inflammasome-related genes that occurs in the absence of such therapy.

In summary, our study suggests the existence of a DNA methylation–mediated control of inflammasome-related genes in monocytes that could contribute to a quick response in an inflammatory environment. These changes are exacerbated in the context of an IL-1β–mediated monogenic autoinflammatory disease, specifically CAPS, perhaps participating in its phenotypic development. Our results highlight the need to further explore these mechanisms and the feasibility of using these epigenetic events as additional biomarkers in the context of autoinflammation.

Key messages

- **Inflammasome-related genes undergo demethylation during macrophage differentiation and monocyte activation.**
- **Demethylation and upregulation of inflammasome genes depends on both TET2 and NF-κB.**
- **Demethylation of inflammasome genes is exacerbated in patients with CAPS, an effect not observed in those patients with CAPS who are treated with anti–IL-1 drugs.**

REFERENCES

1. Geissmann F, Manz MG, Jung S, Sieweke MH, Merad M, Ley K. Development of monocytes, macrophages, and dendritic cells. Science 2010;327:656-61.
2. Serbina NV, Pamer EG. Monocyte emigration from bone marrow during bacterial infection requires signals mediated by chemokine receptor CCR2. Nat Immunol 2006;7:311-7.
3. Fleetwood AJ, Lawrence T, Hamilton JA, Cook AD. Granulocyte-macrophage colony-stimulating factor (CSF) and macrophage CSF-dependent macrophage phenotypes display differences in cytokine profiles and transcription factor activities: implications for CSF blockade in inflammation. J Immunol 2007;178:5245-52.
4. Guo H, Callaway JB, Ting JP. Inflammasomes: mechanism of action, role in disease, and therapeutics. Nat Med 2015;21:677-87.

5. Vanaja SK, Rathinam VA, Fitzgerald KA. Mechanisms of inflammasome activation: recent advances and novel insights. Trends Cell Biol 2015;25: 308-15.
6. Srinivasula SM, Poyet JL, Razmara M, Datta P, Zhang Z, Alnemri ES. The PYRIN-CARD protein ASC is an activating adaptor for caspase-1. J Biol Chem 2002;277:21119-22.
7. Martinon F, Aksentijevich I. New players driving inflammation in monogenic auto-inflammatory diseases. Nat Rev Rheumatol 2015;11:11-20.
8. Hernandez-Rodriguez J, Ruiz-Ortiz E, Tome A, Espinosa G, Gonzalez-Roca E, Mensa-Vilaro A, et al. Clinical and genetic characterization of the autoinflammatory diseases diagnosed in an adult reference center. Autoimmun Rev 2016;15: 9-15.
9. Klug M, Heinz S, Gebhard C, Schwarzfischer L, Krause SW, Andreesen R, et al. Active DNA demethylation in human postmitotic cells correlates with activating histone modifications, but not transcription levels. Genome Biol 2010; 11:R63.
10. Vento-Tormo R, Company C, Rodriguez-Ubreva J, de la Rica L, Urquiza JM, Javierre BM, et al. IL-4 orchestrates STAT6-mediated DNA demethylation leading to dendritic cell differentiation. Genome Biol 2016;17:4.
11. Booth MJ, Ost TW, Beraldi D, Bell NM, Branco MR, Reik W, et al. Oxidative bisulfite sequencing of 5-methylcytosine and 5-hydroxymethylcytosine. Nat Protoc 2013;8:1841-51.
12. Klug M, Schmidhofer S, Gebhard C, Andreesen R, Rehli M. 5-Hydroxymethylcytosine is an essential intermediate of active DNA demethylation processes in primary human monocytes. Genome Biol 2013;14:R46.
13. Martinon F, Petrilli V, Mayor A, Tardivel A, Tschopp J. Gout-associated uric acid crystals activate the NALP3 inflammasome. Nature 2006;440:237-41.
14. Gattorno M, Tassi S, Carta S, Delfino L, Ferlito F, Pelagatti MA, et al. Pattern of interleukin-1beta secretion in response to lipopolysaccharide and ATP before and after interleukin-1 blockade in patients with CIAS1 mutations. Arthritis Rheum 2007;56:3138-48.
15. Giamarellos-Bourboulis EJ, Mouktaroudi M, Bodar E, van der Ven J, Kullberg BJ, Netea MG, et al. Crystals of monosodium urate monohydrate enhance lipopolysaccharide-induced release of interleukin 1 beta by mononuclear cells through a caspase 1-mediated process. Ann Rheum Dis 2009;68:273-8.
16. de la Rica L, Garcia-Gomez A, Comet NR, Rodriguez-Ubreva J, Ciudad L, Vento-Tormo R, et al. NF-kappaB-direct activation of microRNAs with repressive effects on monocyte-specific genes is critical for osteoclast differentiation. Genome Biol 2015;16:2.

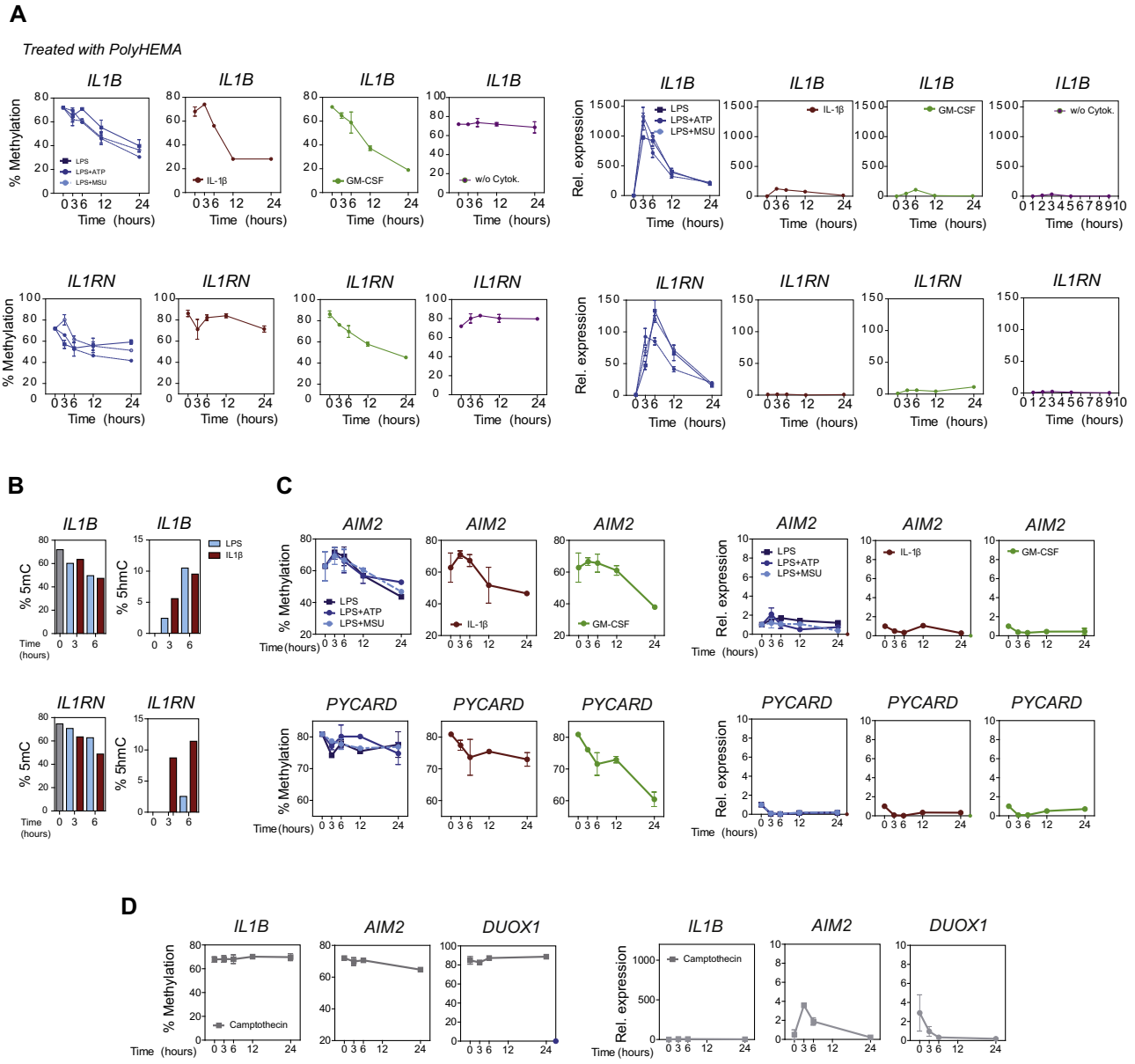

FIG E1. A, Changes in DNA methylation *(left panels)* and expression *(right panels)* of selected inflammasome-related genes (*IL1B* and *IL1RN*) in monocytes stimulated as above in the presence of poly-289 2-hydroxyethyl methacrylate *(polyHEMA)* to prevent attachment to the plates. **B,** Analysis of 5-methylcytosine (*5mC*; *left*) and 5hmC *(right)* of *IL1B* and IL1RN at 0, 3, and 6 hours after treatment with IL-1β and LPS. **C,** *Left panel*, DNA methylation quantified by means of bisulfite pyrosequencing of modified DNA in monocytes cultured after different stimuli over time: LPS, LPS plus ATP, LPS plus MSU (in *blue*), IL-1β (in *red*), and GM-CSF (in *green*) of 2 additional inflammasome-related genes: *AIM2* and *PYCARD*. *Right panel*, Changes in expression of the same genes determined by using qRT-PCR in monocytes cultured under the same conditions described above. **D,** Changes in DNA methylation *(left panel)* and expression *(right panel)* of 2 selected inflammasome-related genes (*IL1B* and *AIM2*) and 1 control gene *(DUOX1)* in the presence of the apoptosis inducer camptothecin.

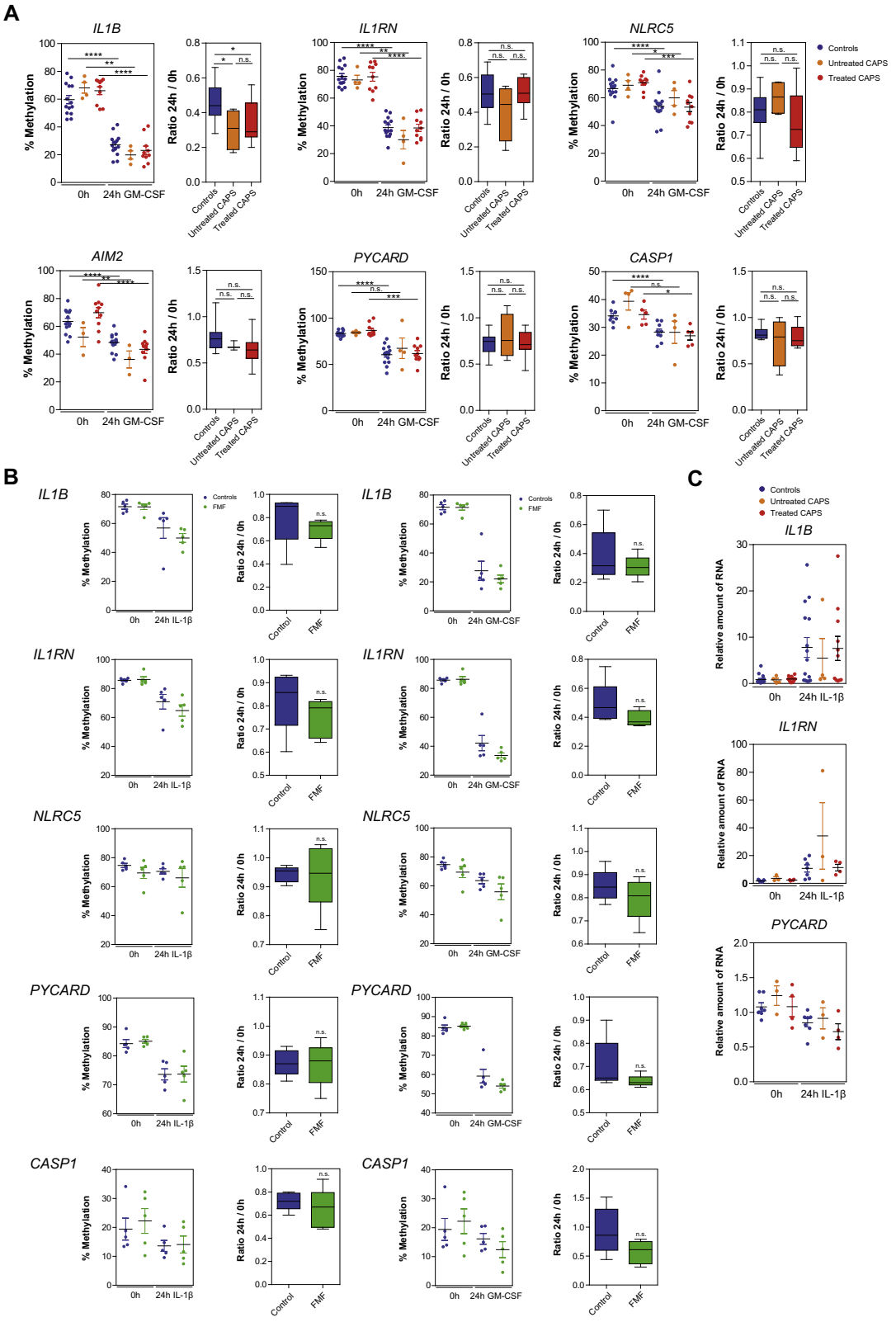

FIG E2. A, Methylation levels of monocytes from patients with CAPS versus healthy subjects of monocytes before (0 hour) and after (24 hours) stimulation with GM-CSF, as estimated by using bisulfite pyrosequencing. For each gene, the ratio between the methylation percentage of monocytes at 24 hours after GM-CSF stimulation and before stimulation is represented. Patients are divided into 2 groups: untreated and treated with anti–IL-1β drugs (details in Tables E2 and E3). **B,** Methylation levels of monocytes from patients with FMF versus healthy subjects before (0 hours) and after (24 hours) stimulation with GM-CSF or IL-1β, as estimated by using bisulfite pyrosequencing. For each gene, the ratio between the methylation percentage of monocytes at 24 hours after stimulation and before stimulation is represented. **C,** Expression data: qRT-PCR for patients with CAPS (untreated/treated with anti–IL-1β drugs) versus healthy subjects. *$P < .05$, **$P < .01$, ***$P < .001$, and ****$P < .0001$.

TABLE E1. List of primers

Primer type	Primer ID	Primer sequence
ChIP	ChIP_hsIL1B_F	GTCTTCCACTTTGTCCCACA
ChIP	ChIP_hsIL1B_R	TGACAATCGTTGTGCAGTTG
ChIP	ChIP_hsIL1RN_F	AAAAGCATATCCTGCTTTGGA
ChIP	ChIP_hsIL1RN_R	CGCTCTAACAAAGGAAAACAGA
ChIP	ChIP_hsIL1A_F	CCTCCTGAATAGCTGGGACT
ChIP	ChIP_hsIL1A_R	GGGTTCCCAGTTGGAGTTTA
ChIP	ChIP_hsCASP1_F	CAAAAGGCAAAAGAGGAGCA
ChIP	ChIP_hsCASP1_R	CTCATGAGATCCGATGGTTTT
ChIP	ChIP_hsMYOD1_F	GTTCCTATTGGCCTCGGACT
ChIP	ChIP_hsMYOD1_R	GCTTCCTCACCCCTAGCTTC
RT-PCR	q_hsDUOX1_F	TTGAGCCCTTCTTCAACTCC
RT-PCR	q_hsDUOX1_R	TTCCACATTCTTGGTCATGC
RT-PCR	q_hsIL1B_F	AGCTGATGGCCCTAAACAGA
RT-PCR	q_hsIL1B_R	GGAGATTCGTAGCTGGATGC
RT-PCR	q_hsIL1A_F	CGGGAAGGTTCTGAAGAAGA
RT-PCR	q_hsIL1A_R	AGGTGCTGACCTAGGCTTGA
RT-PCR	q_hsIL1RN_F	TTGCAAGGACCAAATGTCAA
RT-PCR	q_hsIL1RN_R	AGTGTCTGAGCGGATGAAGG
RT-PCR	q_hsNLRC5_F	AAGCTTTGCCTCTCTGTCCA
RT-PCR	q_hsNLRC5_R	GTGAGGGAGAACCTCCACAA
RT-PCR	q_hsAIM2_F	GCTGCACCAAAAGTCTCTCC
RT-PCR	q_hsAIM2_R	AGCGCTTCTGAAACCCTTCT
RT-PCR	q_hsPYCARD_F	AAGCCAGGCCTGCACTTTAT
RT-PCR	q_hsPYCARD_R	CTGGTACTGCTCATCCGTCA
RT-PCR	q_hsCASP1_F	CTCAGGCTCAGAAGGGAATG
RT-PCR	q_hsCASP1_R	GCGGCTTGACTTGTCCATTA
RT-PCR	q_hsPSTPIP2_F	CCGCAAGAACTGCAAAGAGT
RT-PCR	q_hsPSTPIP2_R	AGACTGTCCACACGGCTTCT
RT-PCR	q_hsMITF_F	ACCATCAGCAACTCCTGTCC
RT-PCR	q_hsMITF_R	TCTCTTTGGCCAGTGCTCTT
RT-PCR	q_hsHPRT1_F	TGACACTGGCAAAACAATGCA
RT-PCR	q_hsHPRT1_R	GGTCCTTTTCACCAGCAAGCT
RT-PCR	q_hsRPL38_F	TGGGTGAGAAAGGTCCTGGTC
RT-PCR	q_hsRPL38_F	CGTCGGGCTGTGAGCAGGAA
BS pyrosequencing	Py_hsDUOX1_F	AGTTTTGGTTTAGGATGTTTTTTAGAAT
BS pyrosequencing	Py_hsDUOX1_R	[BTN]AACAATAACCRAAAATACTAAAACTCCACT
BS pyrosequencing	PySeq_hsDUOX1	TTTAGGATGTTTTTTAGAATTGA
BS pyrosequencing	Py_hsMITF_F	GTTGGGTTGATTTGTGTGGTAT
BS pyrosequencing	Py_hsMITF_R	[BTN]CTTACTATTATTTCAAAACACCACTACC
BS pyrosequencing	PySeq_hsMITF	AGTTGAGTGGAGTAG
BS pyrosequencing	Py_hsIL1B_F	AGGGTTAATTTTTAGTTTTTTTGTTGAGTT
BS pyrosequencing	Py_hsIL1B_R	[BTN] AAACACTACTACTTCTTACCCCCTTTA
BS pyrosequencing	PySeq_hsIL1B	TTATTTTTTTTATTTATTTAAAGTT
BS pyrosequencing	Py_hsIL1RN_F	AGAGTGTTTGGTATATAGGATTAAGT
BS pyrosequencing	Py_hsIL1RN_R	[Btn]AAATAAAACTACCCCTCCTTCCA
BS pyrosequencing	PySeq_hsIL1RN	AGTTTAGTTTTTTGTATGTGATT
BS pyrosequencing	Py_hsIL1A_F	[Btn]ATTTTATAAAGTAAAGGGGTGAATAAATG
BS pyrosequencing	Py_hsIL1A_R	CTCAAACRCCAATAAAATAACTCCCTCTCT
BS pyrosequencing	PySeq_hsIL1A	CTTCTTCRCCTTTTATAATTATCTT
BS pyrosequencing	Py_hsNLRC5_F	GGTTAGGGGAGGTTAAGGTA
BS pyrosequencing	Py_hsNLRC5_R	[Btn]TCCTCTCCCCCTAAACATACTCATC
BS pyrosequencing	PySeq_hsNLRC5	ATTTTGAGTAGGATTTGAAT
BS pyrosequencing	Py_hsAIM2_F	[Btn]AAATTTGGTTGATTGTTGATTTTTAGT
BS pyrosequencing	Py_hsAIM2_R	CACCCTCAAAAAAAAAATACAAACACT
BS pyrosequencing	PySeq_hsAIM2	CACCCTTTTCTTAACTAAAAATA
BS pyrosequencing	Py_hsPYCARD_F	GGTTAGGTTGGTTTTAAATTTTTGATTAT
BS pyrosequencing	Py_hsPYCARD_R	[Btn]TACCACTCRACAACAAACACCTTATCTCA
BS pyrosequencing	PySeq_hsPYCARD	TGGGATTATAGGTATGAG
BS pyrosequencing	Py_hsCASP1_F	GGTGGGTGGTTTATAGTTGTAAT
BS pyrosequencing	Py_hsCASP1_R	[Btn]TCCACCTCCCTAAACTCAAATAATC
BS pyrosequencing	PySeq_hsCASP1	GTGGTTTATAGTTGTAATTTTAGTA
BS pyrosequencing	Py_hsPSTPIP2_F	[Btn]GGAGGGTGATTTAGTTAAAGGTTTAT
BS pyrosequencing	Py_hsPSTPIP2_R	TCCCCATAAAACAAAATATTCTCCTA
BS pyrosequencing	PySeq_hsPSTPIP2	ACCACTAAAATTAAAAAAATATTTC

BS, Bisulfite.

TABLE E2. Features of the patients with CAPS and patients with FMF included in this study

Disease phenotype	Code	Genetic variant (gene/genotype)	Sex	Age at disease onset (y)	Age at time of study (y)	Treatment	Activity
CAPS	CAPS 1	*NLRP3*/p.[(Arg260Trp)];[=]	Male	Early childhood, <1	82	No treatment (azathioprine for kidney transplantation)	Inactive
CAPS	CAPS 2	*NLRP3*/p.[(Arg260Trp)];[=]	Male	Early childhood, <1	48	Anakinra, 100 mg/d	Inactive
CAPS	CAPS 3	*NLRP3*/p.[(Arg260Trp)];[=]	Female	Early childhood, <1	38	Anakinra, 100 mg/d	Inactive
CAPS	CAPS 4	*NLRP3*/p.[(Arg260Trp)];[=]	Female	Early childhood, <1	47	Anakinra, 100 mg/d	Inactive
CAPS	CAPS 5	*NLRP3*/p.[(Arg260Trp)];[=]	Male	Early childhood, <1	55	Anakinra, 100 mg/d	Inactive
CAPS	CAPS 6	*NLRP3*/p.[(Arg260Trp)];[=]	Male	Early childhood, <1	58	Anakinra, 100 mg/d	Inactive
CAPS	CAPS 7	*NLRP3*/p.[(Arg260Trp)];[=]	Female	<1	13	No anti–IL-1 treatment	Inactive
CAPS	CAPS 8	*NLRP3*/p.[(Arg260Trp)];[=]	Female	<1	13	No anti–IL-1 treatment	Inactive
CAPS	CAPS 9	*NLRP3*/p.[(Arg260Trp)];[=]	Female	1	8	No anti–IL-1 treatment	Inactive
CAPS	CAPS 10	*NLRP3*/p.[(Ala439Val)];[=]	Female	4	41	Canakinumab (150 mg/2-3 mo)	Inactive
CAPS	CAPS 11	*NLRP3*/p.[(Ala439Val)];[=]	Female	8	43	Canakinumab (150 mg/2-3 mo)	Inactive
CAPS	CAPS 12	*NLRP3*/p.[(Ala439Val)];[=]	Female	14	56	No specific treatment	Mild symptoms
CAPS	CAPS 13	*NLRP3*/p.[(Ala439Val)];[=]	Male	15	75	Anakinra	Inactive
CAPS	CAPS 14	*NLRP3*/p.[(Ala439Val)];[=]	Female	20	49	Anakinra	Inactive
CAPS	CAPS 15	*NLRP3*/p.[(Ala439Val)];[=]	Female	15	17	Anakinra	Inactive
CAPS	CAPS 16	*NLRP3*/p.[(Ala439Val)];[=]	Male	42	62	Anakinra	Inactive
CAPS	CAPS 17	*NLRP3*/p.[(Ala439Val)];[=]	Male	3	40	Anakinra	Inactive
FMF	FMF 1	*MEFV*/p.[(Met694Val)];[(Val726Ala)]	Male	3	38	Anakinra	Inactive
FMF	FMF 2	*MEFV*/p.[Pro369Ser;Arg408Gln)];[=]	Male	36	40	Colchicine (1.5 mg/d)	Inactive
FMF	FMF 3	*MEFV*/p.[(Met694Val)];[=]	Male	36	49	Canakinumab	Inactive
FMF	FMF 4	*MEFV*/p.[(Met694Ile)];[=]	Male	8	28	Colchicine (1.5 mg/d)	Inactive
FMF	FMF 5	*MEFV*/p.[(Ala744Ser)];[=]	Male	30	39	Canakinumab	Inactive

TABLE E3. Methylation values (percentage methylation obtained by using bisulfite sequencing) of monocytes from patients with CAPS before and after 24 hours of IL-1β and 24 hours of GM-CSF

	Methylation (%)											
Gene:	***IL1B***			***IL1RN***			***NLRC5***			***CASP1***		
Patient code	**MO**	**IL-1β, 24 h**	**GM-CSF, 24 h**	**MO**	**IL-1β, 24 h**	**GM-CSF, 24 h**	**MO**	**IL-1β, 24 h**	**GM-CSF, 24 h**	**MO**	**IL-1β, 24 h**	**GM-CSF, 24 h**
CAPS 1	60.57	35.1	22.9	71.1	58.1	28.8	60.7	47.4	48.1	42.3	38.8	34.3
CAPS 2	68.9	46.2	18.3	75.2	66.7	42.6	71.3	55.6	42.0	39.5	34.8	28.3
CAPS 3	65.0	27.7	19.1	65.0	54.3	33.2	64.0	55.1	42.3	30.9	25.6	23.2
CAPS 4	52.8	28.8	13.5	66.5	56.6	31.3	60.3	54.5	39.0	35.2	27.0	23.7
CAPS 5	55.4	32.2	11.3	67.4	47.1	27.7	69.8	61.3	60.5	36.3	32.8	28.3
CAPS 6	52.7	41.1	22.8	58.5	46.1	36.6	78.7	53.7	53.7	31.1	32.0	31.3
CAPS 7	76.6	58.0	13.0	71.2	48.1	13.1	76.7	65.0	71.0	43.2	20.7	16.5
CAPS 8	63.0	30.0	26.3	67.3	41.9	32.7	72.1	65.8	66.4	41.9	35.3	32.2
CAPS 9	72.2	39.2	17.1	82.6	65.2	45.5	66.8	58.0	54.2	30.0	25.9	29.9
CAPS 10	68.9	28.0	ND	81.0	29.0	ND	65.1	49.9	ND	ND	ND	ND
CAPS 11	68.0	22.1	ND	80.8	45.0	ND	69.0	56.4	ND	ND	ND	ND
CAPS 12	70.0	12.4	ND	80.9	34.3	ND	58.1	38.1	ND	ND	ND	ND
CAPS 13	73.2	55.0	21.5	86.4	62.5	43.9	70.4	68.5	61.2	ND	ND	ND
CAPS 14	55.1	60.7	26.4	82.0	70.6	38.3	72.7	65.8	56.1	ND	ND	ND
CAPS 15	72.0	64.2	38.1	85.9	76.1	51.4	72.8	65.5	71.8	ND	ND	ND
CAPS 16	74.15	63.0	19.6	82.3	69.8	29.9	73.5	76.7	57.7	ND	ND	ND
CAPS 17	72.98	66.0	40.7	84.3	77.4	50.6	75.7	ND	48.7	ND	ND	ND
FMF 1	39.28	55.7	15.2	93.4	75.5	31.9	90.7	77.4	65.9	30.0	20.1	12.7
FMF 2	72.5	56.4	31.2	82.9	68.6	39.2	71.9	73.3	58.2	10.2	9.3	8.1
FMF 3	64.01	46.7	19.0	85.4	57.9	35.8	78.1	73.6	64.6	24.0	11.6	17.0
FMF 4	73.83	40.1	22.8	83.9	53.9	29.9	55.7	41.9	36.2	14.6	7.4	4.6
FMF 5	72.89	50.8	22.1	85.7	67.8	31.5	67.7	64.0	53.5	32.3	22.0	19.7

AIM2			***PYCARD***		
MO	**IL-1β, 24 h**	**GM-CSF, 24 h**	**MO**	**IL-1β, 24 h**	**GM-CSF, 24 h**
39.1	44.2	25.2	81.4	67.5	44.2
56.2	63.4	21.1	85.6	72.1	61.4
48.9	58.2	47.5	80.9	65.2	56.0
62.0	73.8	41.5	100.0	70.5	43.3
68.0	61.2	45.5	81.8	75.7	60.0
89.8	56.6	45.6	96.8	73.5	67.3
ND	ND	ND	86.4	70.4	97.5
54.9	31.0	36.9	84.3	57.3	63.2
62.6	62.9	46.3	84.7	69.9	64.8
65.5	56.7	ND	84.5	79.7	ND
63.3	45.2	ND	83.9	67.7	ND
61.6	37.9	ND	79.2	67.2	ND
73.3	73.4	56.2	89.8	73.6	64.7
77.2	82.1	49.0	82.5	83.3	64.7
75.8	68.5	47.3	82.2	82.6	75.1
76.2	71.2	43.4	84.5	78.0	77.0
70.8	63.6	37.5	83.4	69.8	69.9
51.1	79.9	52.8	84.0	74.9	51.0
73.8	64.6	41.6	84.9	81.6	57.3
72.4	80.6	41.9	86.5	64.6	54.9
68.6	50.2	57.4	86.6	74.4	54.8
77.2	67.3	48.8	83.2	73.1	52.2

Ratio, 24 h/0 h												
IL1B		***IL1RN***		***NLRC5***		***CASP1***		***AIM2***		***PYCARD***	
IL-1β	**GM-CSF**	**IL-1β**	**GM-CSF**	**IL-1β**	**GM-CSF**	**IL-1β**	**GM-CSF**	**IL-1β**	**GM-CSF**	**IL-1β**	**GM-CSF**
0.6	0.4	0.8	0.4	0.8	0.8	0.9	0.8	1.1	0.6	0.8	0.5
0.7	0.3	0.9	0.6	0.8	0.6	0.9	0.7	1.1	0.4	0.8	0.7
0.4	0.3	0.8	0.5	0.9	0.7	0.8	0.8	1.2	1.0	0.8	0.7
0.5	0.3	0.9	0.5	0.9	0.6	0.8	0.7	1.2	0.7	0.7	0.4
0.6	0.2	0.7	0.4	0.9	0.9	0.9	0.8	0.9	0.7	0.9	0.7
0.8	0.4	0.8	0.6	0.7	0.7	1.0	1.0	0.6	0.5	0.8	0.7
0.8	0.2	0.7	0.2	0.8	0.9	0.5	0.4			0.8	1.1

(Continued)

TABLE E3. *(Continued)*

Ratio, 24 h/0 h											
IL1B		*IL1RN*		*NLRC5*		*CASP1*		*AIM2*		*PYCARD*	
IL-1β	GM-CSF	IL-1β	GM-CSF	IL-1β	GM-CSF	IL-1β	GM-CSF	IL-1β	GM-CSF	IL-1β	GM-CSF
0.5	0.4	0.6	0.5	0.9	0.9	0.8	0.8	0.6	0.7	0.7	0.7
0.5	0.2	0.8	0.6	0.9	0.8	0.9	1.0	1.0	0.7	0.8	0.8
0.4		0.4		0.8				0.9		0.9	
0.3		0.6		0.8				0.7		0.8	
0.2		0.4		0.7				0.6		0.8	
0.8	0.3	0.7	0.5	1.0	0.9			1.0	0.8	0.8	0.7
1.1	0.5	0.9	0.5	0.9	0.8			1.1	0.6	1.0	0.8
0.9	0.5	0.9	0.6	0.9	1.0			0.9	0.6	1.0	0.9
0.9	0.3	0.8	0.4	1.0	0.8			0.9	0.6	0.9	0.9
0.9	0.6	0.9	0.6		0.6			0.9	0.5	0.8	0.8
1.4	0.4	0.8	0.3	0.9	0.7	0.7	0.4	1.6	1.0	0.9	0.6
0.8	0.4	0.8	0.5	1.0	0.8	0.9	0.8	0.9	0.6	1.0	0.7
0.7	0.3	0.7	0.4	0.9	0.8	0.5	0.7	1.1	0.6	0.7	0.6
0.5	0.3	0.6	0.4	0.8	0.6	0.5	0.3	0.7	0.8	0.9	0.6
0.7	0.3	0.8	0.4	0.9	0.8	0.7	0.6	0.9	0.6	0.9	0.6

MO, Monocytes; *ND*, not determined.